ELSEVIER

Journal of Hazardous Materials A103 (2003) 205–215

Journal of Hazardous Materials

www.elsevier.com/locate/jhazmat

Shallow layer simulation of heavy gas released on a slope in a calm ambient Part I. Continuous releases

Robin K.S. Hankin*

School of Geography and Environmental Science, The University of Auckland, Private Bag 92019, Glen Innes, Auckland, New Zealand

Received 24 February 2003; received in revised form 4 July 2003; accepted 8 July 2003

Abstract

Although much research considers heavy gas dispersion over flat ground, less is known about the physics of dense gas dispersion on a slope. Here, the appropriateness of shallow layer models for the simple case of releases over a slope in a calm ambient is assessed.

This two-part paper assesses the value of shallow layer modelling using the established shallow layer model TWODEE [J. Hazard. Mater. 66 (3) (1999) 211; J. Hazard. Mater. 66 (3) (1999) 227; J. Hazard. Mater. 66 (3) (1999) 239] and the experimental results of Schatzmann et al. [M. Schatzmann, K. Marotzke, J. Donat, Research on continuous and instantaneous heavy gas clouds, contribution of sub-project EV 4T–0021-D to the final report of the joint CEC project, Technical Report, Meteorological Institute, University of Hamburg, February 1991]. Part I considers continuous releases, and part II considers instantaneous releases; both use the same model with the same entrainment coefficients.

For continuous releases, cloud arrival times are generally well predicted, and cloud concentrations are generally correct to within a factor of two. Shallow layer models thus appear to be capable of physically accurate simulation of continuous releases over a slope in a calm ambient.

Keywords: Heavy gas dispersion; Continuous releases; Shallow layer modelling; Risk assessment; Slopes

1. Introduction

Gravity-driven spreading of fluids is important for many geophysical, industrial, and environmental applications: in particular, the dispersion of gas following a chemical spillage is usually considered in terms of gravity currents [5].

* Present address: Southhampton Oceanography Centre, University of Southhampton, Waterfront Campus, European Way, Southhampton S014 3ZH, UK. Tel.: +44-23-8059-7743
E-mail address: r.hankin@soc.soton.ac.uk (R.K.S. Hankin).

0304-3894/$ – see front matter © 2003 Elsevier B.V. All rights reserved.
doi:10.1016/S0304-3894(03)00224-3

Because they tend to form a low aspect ratio system, gravity currents are well suited to simulation by shallow layer models such as TWODEE [6,1–3]. This model was written to simulate heavy gas dispersion over complex terrain; here it is used to simulate flow over a uniform slope in a calm ambient.

One difficulty that arises when using shallow layer models is the comparison of model output with experimental results: large amounts of data are typically generated by experiments and, in this case, by the model.

Here, I compare TWODEE predictions with the experimental results of Schatzmann et al. [4], in which heavy gas was released over three different slopes in a calm ambient. Continuous releases are considered here; instantaneous releases will be considered in part II of this two-part paper.

1.1. Shallow layer models for dense gas dispersion

In shallow layer modelling of heavy gas clouds, the system is described in terms of depth-averaged variables which vary in (two-dimensional) space and time. The variables are: cloud height h, depth-averaged cloud density $\bar{\rho}$, and two components of depth-averaged velocity $(\bar{u}, \bar{v})$. The following relations are used for *definition* of these four depth-averaged quantities:

$$h(\bar{\rho} - \rho_a) = \int_{z=0}^{\infty} [\rho(z) - \rho_a)]\,\mathrm{d}z$$

$$h(\bar{\rho} - \rho_a)\bar{u} = \int_{z=0}^{\infty} [\rho(z) - \rho_a]u(z)\,\mathrm{d}z$$

$$h(\bar{\rho} - \rho_a)\bar{v} = \int_{z=0}^{\infty} [\rho(z) - \rho_a]v(z)\,\mathrm{d}z.$$

A fourth equation is required to close the system; Hankin [6] showed that it is convenient and meaningful to specify cloud height h as that height below which 95% of the buoyancy is located, viz

$$\int_{z=0}^{h} [\rho(z) - \rho_a]\,\mathrm{d}z = 0.95 \int_{z=0}^{\infty} [\rho(z) - \rho_a]\,\mathrm{d}z.$$

One consequence of adopting a shallow water equation approach to dense gas dispersion is that timescales $\mathcal{T} = \sqrt{h/g'}$ are inaccessible to investigation because the model effectively considers quantities that are averaged over a period $\mathcal{T}$.

1.1.1. The leading edge

These depth-averaged variables evolve according to the standard shallow water equations [1], but with an extra term that ensures that the leading edge moves with a Froude number of unity [1].

If the height of the leading edge is h, and unit vector $\hat{\boldsymbol{n}}$ is normal to the leading edge (write $\boldsymbol{n} = \hat{\boldsymbol{n}}h$), then the total force $\boldsymbol{F}$ exerted by the ambient fluid on the dense layer per

unit width of front will be proportional to $\rho_a h|\boldsymbol{u}_a|^2$; the constant of proportionality k is $2/Fr^2$ where Fr is the front Froude number [6].

The only reasonable vector expressions are:

$$\boldsymbol{F} = \begin{cases} k\rho_a \boldsymbol{u}_a(\boldsymbol{u}_a \cdot \boldsymbol{n}), & [6] \\ k\rho_a \boldsymbol{n}\dfrac{(\boldsymbol{u}_a \cdot \boldsymbol{n})^2}{(\boldsymbol{n} \cdot \boldsymbol{n})}, & [7] \end{cases} \tag{1}$$

where $\boldsymbol{u}_a$ is the velocity of the ambient fluid relative to the front. The work done per unit time per unit width of front by the dense layer on the ambient fluid ($\boldsymbol{F} \cdot \boldsymbol{u}_a$) is identical in each case; the forces differ by $k\rho_a(\boldsymbol{u}_a \cdot \boldsymbol{n})/(\boldsymbol{n} \cdot \boldsymbol{n})\boldsymbol{n} \times (\boldsymbol{u}_a \times \boldsymbol{n})$ per unit width.

1.1.2. Shallow layer models and other types of models

The shallow layer approach is thus a compromise between the complexity of computational fluid dynamics (CFD) models [6] and that of simpler integral models [5]. A CFD model predicts cloud properties over a three-dimensional array of computational elements; its usefulness in the context of dense gas dispersion appears to be uncertain [5]. Integral models describe the cloud in terms of a small number of dependent variables and are discussed, for instantaneous releases over sloping terrain, in part II.

Shallow layer models are particularly well suited to assess the effect of slopes because the downslope buoyancy force is easily included. Entrainment may be incorporated by the use of empirical formulae. Shallow layer models for dense gas dispersion are physically realistic, computationally tractable, and suitable for use in risk assessment [3]; TWODEE compares well with integral models over flat ground for a variety of source terms [8,9].

2. The experiments of Schatzmann et al. [4]

In 1991, Schatzmann et al. [4] investigated the behaviour of heavy gas flowing over a slope. Schatzmann et al. released heavy gas (SF_6, density 6.18 kg m^{-3}) in calm conditions over three different smooth slopes: 4.0, 8.6, and 11.63%. The release point was a gauze-covered orifice, flush with the slope.

Each release lasted for over 70 s and the volume release rate was 2.8×10^{-5} m^{3}s^{-1}; the continuous release experiments were carried out once for each slope. The concentration sensors used were artificially aspirated hot-film anemometers that provided a frequency response of about 50 Hz; gas concentrations could be detected down to about 0.1% (v/v) [10]. The data analysed here were sampled at either 80 or 100 ms intervals. Further details of the experimental setup, and full experimental results in downloadable form, are given by Nielsen and Ott [11].

2.1. Testing models with wind-tunnel data

Model evaluation using wind-tunnel data typically focuses on the difficulties of reproducing the characteristics of atmospheric turbulence [12,13].

Because the experimental data used here required calm conditions, such considerations are immaterial and Britter [5] suggests that laminarization of the plume might become important. Even for the lowest slope, using observed plume densities and predicted plume heights, the Reynolds number $Re \sim h\sqrt{g'h}/\nu \simeq 2000$, suggesting that laminarization is unlikely to occur in the trials.

3. Statistics for continuous releases

There are two physical quantities that are appropriate for describing continuous releases:

Cloud arrival time: Most concentration traces in the experiments show a rapid increase from sensor noise levels to a large value, but some traces do not exhibit such clear-cut behaviour and an objective definition is required.

Cloud arrival time t_a will be defined as the first time at which the cloud concentration exceeds half the maximum concentration of the trace. This definition is generally robust, as the concentration trace usually increases sharply around $t = t_a$.

Average cloud concentration: The continuous traces on Fig. 2 show that 'average' concentration is not an unambiguous concept. The cloud concentration used in this work is the time-averaged concentration C_a for times $t > t_a$, where the system appears to have reached a steady state.

3.1. Goodness-of-fit measures for continuous releases

A 'goodness-of-fit measure' (GFM) is a quantity that expresses how closely a model's predictions match observed values. A smaller GFM generally indicates a better fit (except for the non-parametric FAC2, defined below).

A small GFM can obscure serious shortcomings in a model [6]. Physical interpretation of a model's results must also be made, even though such considerations cannot be objective.

Hanna et al. [14] defined the geometric mean bias MG, the geometric variance VG, and FAC2 in terms of the observed and predicted concentrations C_o and C_p as follows:

$$\mathrm{MG} = \exp[\overline{\ln(C_o/C_p)}]$$
$$\mathrm{VG} = \exp[\overline{\ln(C_o/C_p)^2}]$$
$$\mathrm{FAC2} = \text{fraction of } C_p \text{ within a factor of 2 of } C_o$$

where an overbar denotes averaging over all sensors. Thus, a 'perfect' model would have $\mathrm{MG} = \mathrm{VG} = \mathrm{FAC2} = 1$, although Britter [15] points out that VG is bounded below by stochastic uncertainty and data errors; this issue is addressed more completely under part II of this two-part paper which will cover instantaneous releases.

4. Results and discussion for continuous releases

The three continuous release experiments conducted by Schatzmann et al. [4] were simulated using TWODEE. Fig. 1 shows a plan view of the predicted flow over the 8.6% slope.

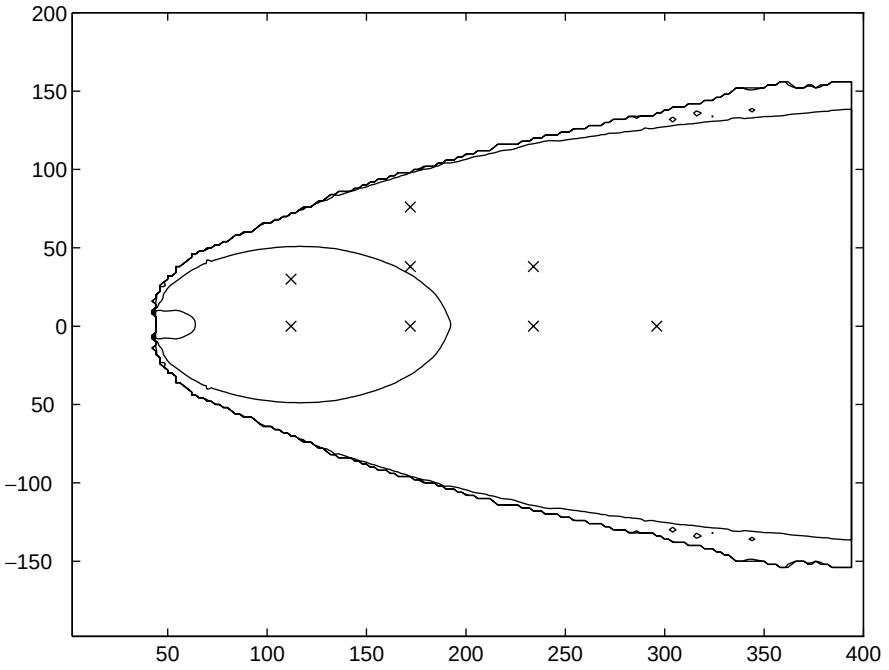

Fig. 1. Contour plot of predicted concentration (values 10, 1, 0.5 and 0.1%) for a continuous release on an 8.6% slope, source at (50, 0). Crosses mark sensor positions; current flows down from left to right.

4.1. Cloud concentrations

Table 1 lists predicted and observed concentrations, at each sensor position. The VG values compare favourably than those obtained at Thorney Island [3], where VG $\simeq 4$.

The model underpredicts slightly, in contrast to the overprediction seen when simulating the Thorney Island releases [6,1]. This discrepancy is possibly a result of the different mechanisms of turbulent entrainment in the outdoor clouds at Thorney Island and the calm ambient releases considered here. Table 1 shows that, for each centreline sensor, increasing slope gives monotonically increasing experimental concentrations, but monotonically decreasing predictions. Possible reasons for this reverse trend are discussed below.

The decreased concentration at ground level for steeper slopes is related to the widening flow pattern. In the one-dimensional flow considered by Ellison and Turner [16], the depth-averaged concentration is inversely proportional to the entrainment coefficient E. Ellison and Turner, although employing slightly different depth averaging techniques and concentrating on slopes steeper than 10° (about 18%), present evidence to suggest that $E \propto \theta$, where θ is the slope. This implies that the depth-averaged concentration *decreases* with increasing slope. Two reasons for the observed trend might be:

(1) The shape parameter S_1 is a function of slope and, while this does not affect the depth-averaged concentration of the flow, the ground level concentration is inversely

Table 1
Coordinates, and observed and predicted concentrations for all nine sensors in each of Schatzmann et al.'s three continuous release experiments

Coords/slope (%)	Concentrations (%, obs vs. pred)		
	4	8.6	11.63
(61, 0)*	$5.49 > 2.71$	$6.04 > 2.21$	$6.91 > 2.10$
(61, 31)	$2.09 \lesssim 2.50$	$1.21 \lesssim 1.90$	$0.77 < 1.60$
(123, 0)*	$2.58 \gtrsim 1.43$	$3.17 > 1.03$	$3.67 > 0.92$
(123, 23)	n/a	n/a	$2.02 > 0.88$
(123, 38)	$1.10 \lesssim 1.35$	$0.90 \lesssim 0.94$	$0.66 \lesssim 0.77$
(123, 77)	$0.43 < 1.15$	$0.18 < 0.67$	n/a
(184, 0)*	$1.62 \gtrsim 0.93$	$1.93 > 0.64$	$2.22 > 0.56$
(184, 38)	$1.02 \gtrsim 0.92$	$0.99 \gtrsim 0.61$	$1.02 > 0.50$
(245, 0)*	$1.39 \gtrsim 0.72$	$1.44 > 0.47$	$1.71 > 0.39$
	GFMs: all sensors		
MG	1.17	1.46	2.14
VG	1.39	2.37	3.15
FAC2	0.75	0.38	0.12
	GFMs: centreline sensors		
MG	1.87	2.96	3.88
VG	1.48	3.27	6.37
FAC2	0.75	0	0

Measurements in cm; source at $(0, 0)$; $*$ denotes a centreline sensor. Here, "$\lesssim$" and "$\gtrsim$" mean "correct to within a factor of two". For example "$2.09 \lesssim 2.50$" means that the observed concentration of 2.09% is less than the predicted 2.50% but correct to within a factor of two.

proportional to S_1 [6]. Here, S_1 is that used by Ellison and Turner [16]: $1/2(\bar{\rho}-\rho_a)h^2 = S_1 \int_{z=0}^{\infty}(\rho(z) - \rho_a)z\,\mathrm{d}z$, where an overline denotes a depth-averaged quantity. Thus, a low value of S_1 indicates that the majority of the excess density of the layer is at heights low compared to the 95th percentile.

(2) Steep slopes affect the two-dimensional structure of the flow and in particular inhibit the outward spread of fluid from the source.

Both these phenomena occur to some extent, but neither is directly detected in the experiments.

Fig. 2 shows the concentration trace for each slope at the point (184, 0). If the intermittent noise on the 4% trace is ignored, it may be seen that an increase in slope is associated with a higher average concentration. Although the trace for the 11.63% slope appears to increase less abruptly than the shallower slopes, this is not necessarily significant as this feature is not seen elsewhere.

4.2. Cloud arrival times

Table 2 shows predicted and observed cloud arrival times. It may be seen that arrival time is quite well predicted on the centreline, for each sensor position. Off-axis sensors are less well predicted, and arrival times are typically early.

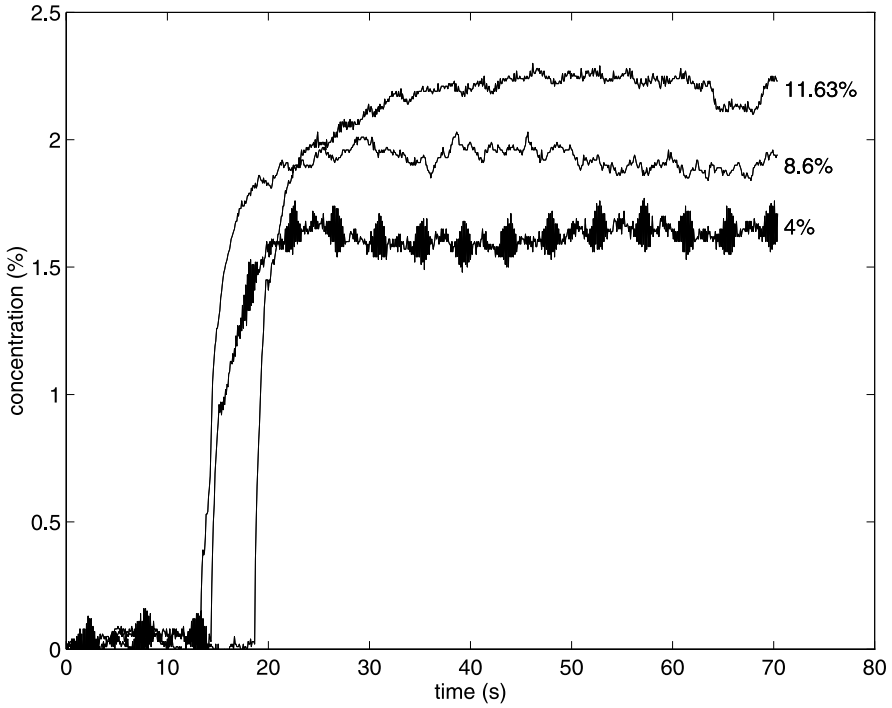

Fig. 2. Eulerian concentration traces for the sensor at (184, 0) for each slope.

The pattern at 123 cm downslope distance is consistent over all three slopes: the residual (observed minus predicted) arrival time increases monotonically with distance from centerline. This is consistent with the simulated cloud front being too pointed because off-axis sensors encounter gas increasingly late.

At present, it is not clear whether the observed cloud arrival times support the view of Webber et al. [7], or that of Hankin [1] (Eq. (1)). Further work on oblique gravity current fronts on slopes would be needed to assess the leading edge condition used in TWODEE.

4.3. Individual concentration traces

Fig. 3 shows the predicted and observed Eulerian concentration trace at (61, 0). This figure is typical in three respects:

(1) Cloud arrival time is well predicted on the centreline. This is evidence that the boundary conditions used in TWODEE [6,1] are appropriate. However, the late arrival time generally seen for off-axis sensors may be due to poor simulation of the three-dimensional flow behind the leading edge.
(2) The mean concentration is underpredicted by a factor of about 3. In this context, underprediction of the mean concentration at ground level is associated with the vertical profile used. Here, an exponential profile is used but alternative profiles will give

Table 2
Coordinates, and observed and predicted cloud arrival times for all nine sensors in each of Schatzmann et al.'s three continuous release experiments

Coords/slope (%)	Arrival time (s, obs vs. pred)		
	4	8.6	11.63
(61, 0)*	9.9 > 7.5	6.0 < 6.1	9.8 > 5.8
(61, 31)	12.9 > 9.5	9.0 > 8.4	13.3 > 7.7
(123, 0)*	20.4 > 15.6	12.1 < 12.2	14.2 > 11.3
(123, 23)	n/a	n/a	15.8 > 11.6
(123, 38)	24.4 > 17.2	14.6 > 13.9	18.8 > 13.1
(123, 77)	34.2 > 23.4	35.8 > 21.0	n/a
(184, 0)*	28.2 > 24.2	18.1 < 18.6	19.4 > 17.1
(184, 38)	34.3 > 24.6	20.7 > 19.2	23.7 > 18.0
(245, 0)*	35.5 > 33.2	24.0 < 25.3	25.7 > 23.0
	GFMs: all sensors		
MG	1.30	1.08	1.36
VG	1.08	1.03	1.13
FAC2	1	1	1
	GFMs: centreline sensors		
MG	1.21	0.97	1.28
VG	1.05	1.00	1.09
FAC2	1	1	1

Measurements in cm; source at (0, 0); ∗ denotes a centreline sensor.

different results [6]. The dependence of the predicted steady-state concentration on the entrainment parameters used in TWODEE is discussed below in Section 4.4.

(3) Unlike the experimental trace, the predicted trace rises to a maximum before stabilizing. This phenomenon occurs nowhere in the experimental results and is a result of the non-steady flow immediately after starting (TWODEE, being a time-dependent model, simulates this non-steady starting phase). The magnitude of the peak decreases with increasing distance from source; no similar peak is observed at the furthest points.

Interpretation of point 3 above is difficult. It appears to be due to a mismatch between the leading edge and the following flow, suggesting an inappropriately small front Froude number; but as cloud arrival times are quite accurately predicted, this would not seem to be the case. This could be due to shallow layer models not being able to include edge entrainment [6].

The initial high concentration (Fig. 3) is associated with a localized region of low cloud height and relatively high concentration. This region is created immediately after the buoyancy flux starts, and travels in front of the leading edge. Although this heavy fluid disperses slowly (the following flow gradually overtakes and merges with it), Eulerian concentration histories show its presence.

It is reasonable to conjecture that the quasi-equilibrium analysis used to motivate the leading edge condition of TWODEE [6,1] is not strictly applicable: the experimental flow reverts to equilibrium faster than the simulation. This might be expected because depth-averaged

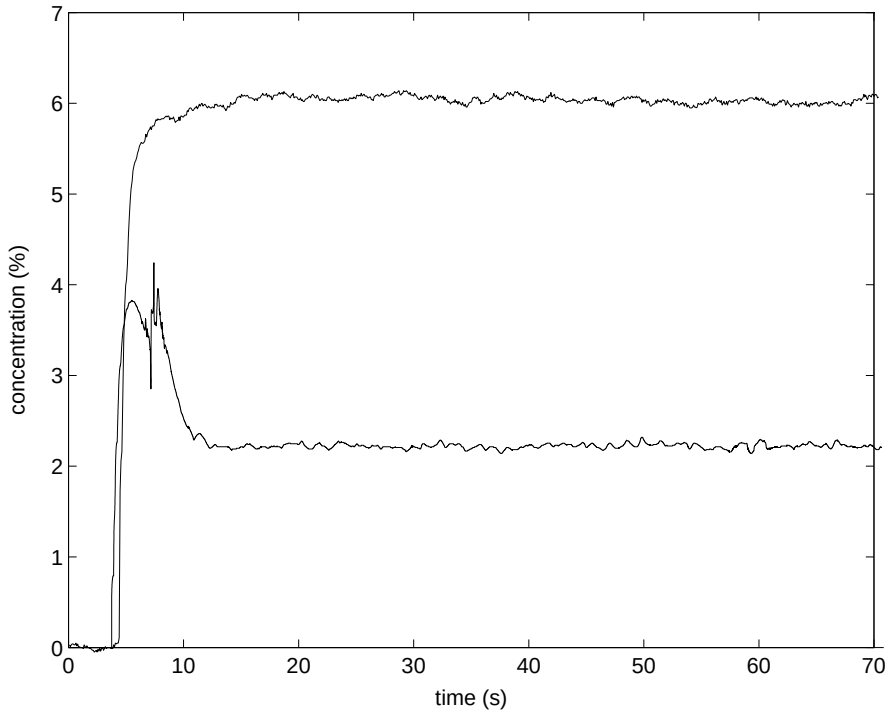

Fig. 3. Predicted (lower) and experimental (upper) Eulerian concentration traces for the sensor at $(61, 0)$ on the 8.6% slope.

quantities are used in TWODEE, while the experimental flow generally has a multi-layer structure that allows faster adjustment to a state of quasi-equilibrium.

4.4. Entrainment in shallow layer models

The preceding discussion has presented some of the issues that are present when using shallow layer models to simulate continuous releases in a calm ambient.

In the indoor experiments of Schatzmann et al. [4], the ambient fluid was at rest so turbulence was generated internally, at the shear layer. In contrast, at Thorney Island, the main source of turbulent kinetic energy in the atmosphere, and characterized in TWODEE as the friction velocity u_*. This was described by Turner [17] as externally generated turbulence.

TWODEE incorporates a commonly used [5,18,19] entrainment formula:

$$w_\mathrm{t} = \frac{a}{1 + b\,Ri} v \tag{2}$$

where w_t is the top entrainment velocity, a and b the experimentally determined coefficients [6,1,3], v a representative velocity scale, and $Ri = g'h/v^2$ the Richardson number. The velocity scale v used in TWODEE is a quadratically weighted sum:

$$v^2 = u_*^2 + (\alpha_2 w_*)^2 + \tfrac{1}{2} C_\mathrm{D} \alpha_3^2 \boldsymbol{u}^2 + \alpha_7^2 |\boldsymbol{u} - \boldsymbol{u}_\mathrm{a}|^2$$

Here u_* and v_* are the friction velocity and Monin–Obukov velocity respectively, C_D a roughness coefficient for the ground, and $\boldsymbol{u}$ and $\boldsymbol{u}_a$ the layer velocity and ambient velocity, respectively. The α terms are free parameters, following Eidsvik's [20] notation.

From Table 1, a case could be made to reduce the relative layer speed weight α_7. However, results for the instantaneous case, presented in part II of this two-part paper, would not support this argument.

Fig. 3, showing under prediction by a factor of about 3, might be interpreted as evidence to increase the value of a in Eq. (2). However, this would further increase the overprediction as measured by MG; and if predicted concentrations increased uniformly, this would further degrade VG.

5. Summary

The continuous release results of Schatzmann et al. [4] were analysed using the TWODEE shallow layer model.

TWODEE simulated these experiments and gave useful output. Concentrations were generally underpredicted. Cloud arrival times were quite accurate for centreline sensors and late for off-axis sensors.

Both formal statistical methods and physical reasoning were used to assess the model's performance.

This paper has shown that shallow layer modelling is appropriate for continuous releases of heavy gas over a slope in a calm ambient.

References

[1] R.K.S. Hankin, R.E. Britter, TWODEE: the Health and Safety Laboratory's shallow layer model for dense gas dispersion. Part I. Mathematical basis and physical assumptions, J. Hazard. Mater. 66 (3) (1999) 211–226.
[2] R.K.S. Hankin, R.E. Britter, TWODEE: the Health and Safety Laboratory's shallow layer model for dense gas dispersion. Part II. Outline and validation of the computational scheme, J. Hazard. Mater. 66 (3) (1999) 227–237.
[3] R.K.S. Hankin, R.E. Britter, TWODEE: the Health and Safety Laboratory's shallow layer model for dense gas dispersion. Part III. Experimental validation (Thorney Island), J. Hazard. Mater. 66 (3) (1999) 239–261.
[4] M. Schatzmann, K. Marotzke, J. Donat, Research on continuous and instantaneous heavy gas clouds, contribution of sub-project EV 4T–0021-D to the final report of the joint CEC project, Technical report, Meteorological Institute, University of Hamburg, February 1991.
[5] R.E. Britter, Atmospheric dispersion of dense gases, Ann. Rev. Fluid Mech. 21 (1989) 317–344.
[6] R.K.S. Hankin, Heavy gas dispersion over complex terrain, Ph.D. Thesis, Cambridge University, Cambridge, 1997.
[7] D.M. Webber, S.J. Jones, D. Martin, A model of the motion of a heavy gas cloud released on a uniform slope, J. Hazard. Mater. 33 (1993) 101–122.
[8] R.K.S. Hankin, Comparison of the TWODEE model against the Mercer et al., heavy gas dispersion code comparison exercise, Technical report RAS/96/19, Health and Safety Laboratory, Broad Lane, Sheffield S3 7HQ, 1996.
[9] R.K.S. Hankin, Heavy gas dispersion: integral models and shallow layer models, J. Hazard. Mater., in press.
[10] G. König, M. Schatzmann, A. Lohmeyer, Measurements of gas concentration fluctuations in wind tunnel simulations, in: Proceedings of the 7th International Conference on Wind Engineering, Aachen, FRG, International Association for Wind Engineering, July 1987.

[11] M. Nielsen, S. Ott, A Collection of data from dense gas experiments, Technical report Risø-R-845(EN), Risø National Laboratory, Roskilde, Denmark, March 1996.
[12] R.E. Britter, J. McQuaid, Workbook on the dispersion of dense gases, HMSO, 1988.
[13] W.L. Sweatman, P.C. Chatwin, Dosages from instantaneous releases of dense gases in wind tunnels and into a neutrally stable atmosphere, Bound. Layer Meteorol. 77 (1996) 211–231.
[14] S.R. Hanna, J.C. Chang, D.G. Strimaitis, Hazardous gas model evaluation with field observations, Atmos. Environ. 27A (15) (1993) 2265–2285.
[15] R.E. Britter, The evaluation of technical models used for major-accident hazard installations, report to Commission of the European Communities Directorate General XII, Technical report, Department of Engineering, University of Cambridge, Trumpington Street, Cambridge CB2 1PZ, UK, 1991.
[16] T.H. Ellison, J.S. Turner, Turbulent entrainment in stratified flows, J. Fluid Mech. 6(3) (3) (1959) 529–544.
[17] J.S. Turner, Buoyancy effects in fluids, Cambridge University Press, Cambridge, 1979.
[18] H. Kato, O.M. Phillips, On the penetration of a turbulent layer into a stratified fluid, J. Fluid Mech. 37 (1969) 643–655.
[19] O. Zeman, H. Tennekes, Parametrization of the turbulent energy budget at the top of the day-time atmospheric boundary layer, J. Atmos. Sci. 34(1) (1) (1977) 111–123.
[20] K.J. Eidsvik, Dispersion of heavy gas clouds in the atmosphere, Technical Report No. 32/78; 25077, Norwegian Institute for Air Research, P.O. Box 130, 2001 Lillestrøm, Norway, 1978.